Comparing steady counterflow separation with differential chromatography

Donald K. Roper* and Edwin N. Lightfoot

1415 Johnson Drive, Department of Chemical Engineering, University of Wisconsin-Madison, Madison, WI 53706 (USA)

ABSTRACT

Separation of closely related solutes by steady solid–fluid counterflow is compared with differential separation in a fixed chromatographic bed. Analogous expressions for exit concentration and mean residence time in the two systems are presented. A counterpart to chromatographic resolution is derived for binary steady counterflow separations. Estimated counterflow savings in product-concentration dilution, solvent volume requirement and solid-phase volume requirement obtained with these expressions relative to comparable chromatographic operations are compared with experimental results from adsorptive, simulated moving beds. Analysis of a size-exclusion protein separation suggests counterflow substantially decreases solvent and resin usage relative to conventional, batch operation.

INTRODUCTION

Our purpose in this work is to compare the separation of closely related solutes by steady counterflow of a carrier liquid and an adsorptive solid with the performance expected from comparable fixed-bed chromatography. We are motivated by reports which indicate that reduced solvent and adsorbent volumes are required in experimental simulated-counterflow systems relative to conventional batch adsorption.

Perhaps the most attractive method of achieving steady counterflow without moving a granular bed is to adopt the simulated moving-bed strategy first described by Broughton *et al.* [1] at Universal Oil Products for a continuous para-xylene (PAREX) separation. Movement of solid adsorbent counter to fluid feed and desorbent streams was simulated by intermittently switching feed, extract and raffinate points in the direction of fluid flow using a patented rotary valve. These authors reported simulated-counterflow extraction of 98.5% of one component in a hypothetical binary mix at 99.5% purity decreased adsorbent inventory 25-fold and halved desorbent circulation relative to fixed-bed operation.

This strategy has been adopted in a number of Sorbex-type systems. Recently, Negawa and Shoji [2] reported that to resolve racemic 1-phenylethanol to 99% enantiomeric excess, 87 times less solvent volume per gram of product was required by simulated counterflow than by batch chromatography. The measured adsorbent productivity of counterflow, (calculated as grams of product per hour per liter of bed) was 61 times higher than that of chromatography. Rossiter and Tolbert [3] reported an average ten-fold reduction in adsorbent inventory and roughly 50% reduction in elution volume when simulated-counterflow contacting replaced ion-exchange batch adsorption of amino and carboxylic acids. Relative savings in adsorptive costs upon switching to solid–fluid counterflow were noted by Ernst and McQuigg [4] for recovery of

---

* Corresponding author.

citric and lactic acid from crude fermentation broths.

But early comparisons of model countercurrent and chromatographic separations have not anticipated order-of-magnitude decreases in adsorbent volume and substantial reductions in solvent volume which are indicated by these reports. Liapis and Rippin [5] reported a three-fold relative increase in counterflow carbon-adsorbent utilization after numerically simulating non-linear, binary separations in three modes: batch, periodically switched and continuous-countercurrent operation. In their model, orthogonal collocation was used along the particle radii and along the bed axis in a differential model to account for convective axial dispersion, film resistance to mass transfer, and intraparticle diffusion. Ruthven [6] predicted a four-fold adsorbent volume reduction in staged-counterflow relative to batch chromatography for linear systems with equivalent net solute flow-rates and separation factors of 1.1 which yielded 99% fractional purity. The staged-counterflow internal solute reflux in this model was minimized while the fixed-bed production rate was maximized.

Effort has been dedicated in previous modelling of linear and non-linear counterflow systems to obtain and verify intracolumn concentration profiles from underlying equilibrium and mass transfer processes. Lapidus and Amundson [7] calculated analytic expressions for equilibrium stage composition of a single component from an unsteady-state, difference model of two-phase, linear counterflow separation. Miyauchi and Vermeulen [8] derived pointwise concentration profiles from a steady-state, differential description. Subsequent analyses which considered effects of non-linear equilibria, mass-transfer resistances, multicomponent adsorption and periodic switching have been summarized by Ruthven and Ching [9]. Modelling of separations in simulated moving-bed counterflow by Ernst and Hsu [10] and Storti *et al.* [11] and in continuous moving-bed counterflow by Fish *et al.* [12] have recently been reported. In the chromatographic literature, models giving effluent peaks for a range of systems have been detailed

by Giddings [13], Aris and Amundson [14], Ruthven [6], Lin *et al.* [15] and others.

Rather than emphasizing concentration profiles, our objective in this work has been to address these practical questions: (i) what is the basis for substantial apparent decreases in solvent and adsorbent usage obtained by simulating counterflow?, (ii) how do the relative gains which have been reported compare with those expected from ideal chromatographic and counterflow systems?, and (iii) is the anticipated increase in performance sufficient to justify replacing a particular chromatographic separation with a simulated-counterflow split?

We begin by comparing reliable descriptions of chromatography and steady counterflow of sufficient detail to analyze reasons for the improved efficiency of simulated moving-bed separations. We then derive general expressions to estimate the volumes of solvent and solid resin required by steady counterflow relative to the corresponding volumes required by differential chromatography for difficult, binary separations of equal resolution. We measure the performance of experimental systems, including separations of solutes whose isotherms are non-linear, using these expressions. We conclude by comparing counterflow and chromatography in a hypothetical separation of two proteins.

SEPARATION IN STEADY COUNTERFLOW AND DIFFERENTIAL CHROMATOGRAPHY

We now summarize analytic relations for exit composition, solute mean residence time and binary resolution in analogous chromatographic and counterflow separations, beginning with chromatography. Other than an equation for separation effectiveness in binary counterflow which we derive in the *Binary counterflow separation* section, these relations have been established by previous investigators and we briefly review pertinent literature as they are introduced. For clarity we define the parameters of the relations in context. We will subsequently use these relations to determine the basis for a steady counterflow advantage and to derive

D.K. Roper and E.N. Lightfoot / J. Chromatogr. A 654 (1993) 1–16

3

expressions for the performance of counterflow relative to chromatography.

Differential chromatography

A lumped-parameter, asymptotic solution to one-dimensional, pseudocontinuum equations of differential chromatography in linear systems was obtained by Reis et al. [16] for rapid adsorption and later extended by Gibbs and Lightfoot [17] to account for adsorption kinetics and to examine gradient elution. This solution can be extended using the principle of superposition to describe batch adsorption and elution [18]. Athalye et al. [19] have recently demonstrated the predictability of protein separations in commercially available size-exclusion systems using this model, together with independent, a priori estimates of three transport rate parameters: the convective dispersion coefficient, the intraparticle diffusivity and the fluid-phase mass-transfer coefficient.

Fundamental mass-transport rate processes —convection, diffusion and adsorption— underlie linear systems as well as those in which nonlinearities arise due to concentration-dependence of transport parameters and solute–solute interactions. For this reason, evaluation of steady counterflow efficiency relative to fixed-bed chromatography in linear systems is a useful first step to predicting and optimizing separation performance in more complex operations.

In Table I the fluid-phase solute concentration distribution c_f from a sharp-pulse input of solute mass m_0 which is eluted isocratically in a long column is given as a function of axial coordinate z and time t. The mean solute position, $z_0 \equiv uvt$, is proportional to both the interstitial fluid velocity, v, and the fraction of solute in the moving fluid phase at long times, $u \equiv \alpha\epsilon_b/[\alpha\epsilon_b + (1 - \epsilon_b)]$, where ϵ_b is the interparticle or column void fraction. The column cross-sectional area is A. Increases in H, the height of a theoretical chromatographic plate N, with velocity have been estimated using coefficients of physical transport rate processes. Subscripts f and b refer to the moving fluid and stationary bulk phases, respectively. The bulk phase consists of chromatographic packing of porosity ϵ_p, which entrains fluid referred to by subscript p'.

The differential separation of two individual solutes, distinguished by their respective equilibrium and mass transport rate parameters, is

TABLE I

SUMMARY OF ANALOGOUS RELATIONS FOR STEADY COUNTERFLOW AND DIFFERENTIAL CHROMATOGRAPHY

Relation	Differential chromatography	Steady counterflow
Exit Composition	$c_f(z, t) = \dfrac{m_0 u}{A\epsilon_b\sqrt{2\pi H z_0}} \exp\left[\dfrac{-(z - z_0)^2}{2H z_0}\right]$	$y_{N,i} = \dfrac{y_{e,i}}{\sum_{j=0}^{N} \Gamma_i^{-j}}$
		$x_{1,i} = \dfrac{y_{e,i}}{\alpha_i \dfrac{\rho_S}{\rho_U} \sum_{j=0}^{M} \Gamma_i^j}$
Residence time	$\bar{t} = \dfrac{NH}{uv}$	$\bar{t}_F = \dfrac{H_{SC}(N_{SC} + 1)}{uv_{SC}}\left[\dfrac{\Gamma}{\Gamma - 1} \cdot \dfrac{\Gamma^{N_{SC}+1} - 1}{\Gamma^{N_{SC}+1} + 1}\right]$
Resolution	$R = \dfrac{\delta\sqrt{N}}{4}$	$N_{SC,tot} = 2\left[\dfrac{2\ln\left(\dfrac{P_{U,i}}{1 - P_{U,i}}\right)}{\delta} - 1\right] + 1$

illustrated in Fig. 1. Observe that only a small fraction of the adsorbent bed actively resolves the overlapping solutes. The remainder acts as expensive storage or is unused (frontal and displacement operations are qualitatively similar). Each solute partitions between fluid and bulk phases thermodynamically as shown by its partition coefficient, $\alpha \equiv c_f/c_b = 1/[\epsilon_{p'} + (1 - \epsilon_{p'})K_{eq}]$, with a constant equilibrium distribution coefficient defined by $K_{eq} \equiv k_{ad}/k_{des} = c_s/c_p$. Subscript s refers to the surface of the porous packing, while k_{ad} and k_{des} are kinetic rate constants for adsorption and desorption, respectively.

The solute mean residence time, $\bar{t}$, given in Table I is the first temporal moment of the fluid-phase solute concentration at the column outlet, $z = L$. The second central temporal moment (variance), $s^2 \equiv \bar{t}H/uv$, is the measured width of a peak in Fig. 1. It is proportional to both the residence time and the chromatographic

plate height. Evaluation of temporal moments of c_f is straightforward, because this distribution approaches Gaussian form in time when evaluated at a given coordinate as the number of theoretical chromatographic plates becomes large. Van Deemter [20] obtained equivalent relations for mean residence time and peak width from an equilibrium-plate, continuous-flow description of linear chromatography. Karol [21] derived identical relations from a staged, intermittent-transfer description in which $u_i \rightarrow 0$.

The effective separation of similar components 1 and 2, as illustrated in Fig. 1, has been related to specific thermodynamic and transport rate properties by defining the chromatographic resolution as the ratio of peak separation to the average peak width. In Table I we give a relation for resolution in which the thermodynamic driving force for separation is represented by $\delta \equiv 2|u_1 - u_2|/(u_1 + u_2)$, the fractional difference in migration velocities of 1 and 2. This separation
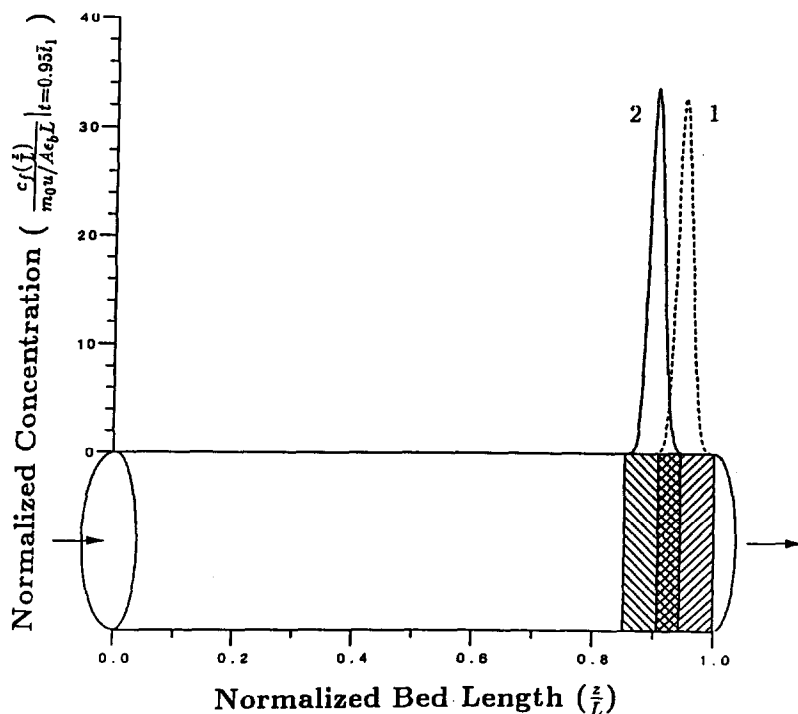

Fig. 1. Underutilization of stationary bed in a binary chromatographic separation. Only 5% of the bed volume (crosshatched) is actively separating component 1 (dashed line) from component 2 (solid line). 9% of the bed volume (hatched) merely retains the eluting species. 86% of the bed is unused. Normalized axial fluid-concentration profiles for 1 and 2 were calculated using the equation for c_f in Table I at $t = 0.95\,\bar{t}_1$. The thermodynamic driving force between 1 and 2 is 0.05. The column illustrated resolves 1 and 2 to unity at $z/L = 1$.

driving force equals the product of relative selectivity and retention factors [22].

We now describe analogous relations from a model of counterflow separation.

Equilibrium-staged counterflow

An equilibrium-stage description of counterflow with constant stage-to-stage phase flow-rates and linear stage-exit equilibrium was introduced by Kremser [23] and Souders and Brown [24] and has been discussed by King [25], Treybal [26] and Henley and Seader [27]. Ruthven [6] showed that an equilibrium-stage approach gives intracolumn profiles which are essentially the same as those from a discrete, one-dimensional, pseudocontinuum description of counterflow. Ching et al. [28] and Ruthven and Ching [9] demonstrated qualitative agreement between concentration profiles calculated using the equilibrium-stage description and measurements from four-section simulated moving-bed experiments. Klinkenberg and co-workers [29,30] specialized the Kremser–Souders–Brown equations to model a column with negligible feed flow-rate relative to the flow-rates of initially pure fluid and solid phases.

In Table I the fluid-phase mass fraction of solute i in the stripper product, $y_{N,i}$, and the solid-phase mass fraction in the enricher product, $x_{1,i}$, are related recursively to the mass fraction of i at a central feed stage, $y_{e,i}$. The model counterflow column consisting of a stripping section of N_{SC} hypothetical stages separated by a single feed stage (subscript e) from an enriching section of M hypothetical stages is sketched in Fig. 2. The extraction ratio, $\Gamma_i \equiv (\alpha_i \rho_S / \rho_U)|U/S|$, summarizes the phase-partitioning of component i at steady mass flow-rates of fluid eluent, $U \equiv (1 - r)\epsilon_b VT$, and solid adsorbent, $S \equiv -r(1 - \epsilon_b)VT$. The volume of one stage is V, T represents the transfer rate of one stage volume, r is the fractional relative motion of the solid phase and ρ_p is the density of phase p. Subscripts U and S refer to the fluid and solid phases, respectively. The fluid-phase mass flow-rate is related to the equivalent countercurrent interstitial liquid velocity, v_{SC}, by $U = A_{SC}\epsilon_b v_{SC} \rho_U$ where A_{SC} is the counterflow-column cross-section.
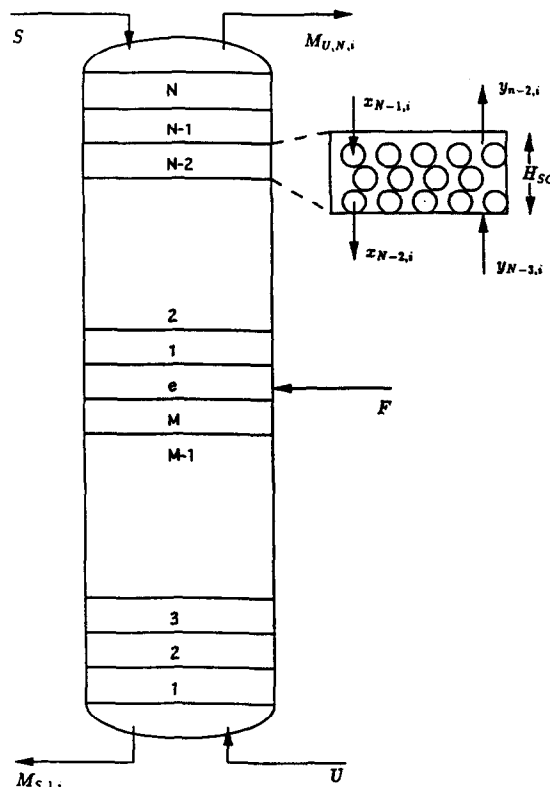

Fig. 2. Equilibrium-stage representation of steady counterflow. The enricher is composed of M stages. N stages comprise the stripper. The feedstream (F) enters stage e. Pure solid (S) and fluid (U) streams enter the stripper and enricher, respectively. The mass flow-rates of component i exiting the column from the stripper ($M_{U,N,i}$) and the enricher ($M_{S,1,i}$) are indicated. Within the column, component i enters and exits a representative stage $j = N - 2$ of height H_{SC} with mass fraction values in the lower solid phase (spheres) ($x_{j,i}$) and upper fluid phase ($y_{j,i}$) as shown.

Solutes 1 and 2 enter the column dissolved in liquid eluent at the feed stage and are completely equilibrated on each stage j so that exiting fluid and solid mass fractions are related: $y_{j,i} = \alpha_i x_{j,i} \rho_S / \rho_U$. Ruthven [6] used a pseudocontinuum description of counterflow to relate the height of a steady counterflow stage, H_{SC}, to operating conditions as well as to individual contributions of microscopic, mass-transfer rate processes in difficult separations.

The solute mean residence time in counterflow, $\bar{t}_F$, given in Table I has been evaluated by taking the temporal first moment of the dynamic response to an impulse injection [31]. Subscript F refers to the feedstream. An identical relation

for mean residence time was derived by these authors, following Buffham and Kropholler [32], by calculating the ratio of total solute inventory to throughput in a steady counterflow system.

We now derive the relation for separation effectiveness in steady counterflow given in Table I.

Binary counterflow separation

A compact, analytical equation analogous to chromatographic resolution which relates separation by steady counterflow to specific thermodynamic (δ) and transport rate properties (reflected in H_{SC} or equivalently, in N_{SC}) is not available from the literature. Our derivation of this equation follows. We first relate fractional purity in an optimally operated column to the extraction ratio and the number of equilibrium counterflow stages using the counterflow mass ratio. We then express the extraction ratio in terms of the thermodynamic driving force to obtain the desired relation.

The fractional purity $P_{p,i}$ of species i leaving a counterflow column in phase p may be written in terms of corresponding solute mass flow-rates as

$$P_{p,i} = \frac{M_{p,j,i}}{M_{p,j,i} + M_{p,j,h\neq i}} \quad (1)$$

where the mass flow-rate of solute i leaving stage j in phase p, $M_{p,j,i}$, is the product of a solute mass fraction and its corresponding phase flow-rate *i.e.* $M_{U,j,i} \equiv Uy_{j,i}$. For fractional purity in the exiting upper liquid phase, the exit-stage subscript j equals N and the phase subscript p equals U. By way of comparison, fractional purity achieved in differential chromatography can be approximated as

$$P = \int_{(\bar{t}_1 + \bar{t}_2)/2}^{\infty} \frac{A\epsilon_b v c_f(t)|_{z=L}}{m_0} \, dt \approx \Phi(2R) \quad (2)$$

where the Gaussian nature of the effluent concentration suggests writing this integral as a cumulative distribution function, Φ, described by Hogg and Ledolter [33]. The argument of this function simplifies to $2R$ since ideal mean residence times and distributional variances of similar solutes are nearly equal. The fractional purity corresponding to a chromatographic resolution,

R can be obtained from tabulated values of $\Phi(2R)$.

The species mass flow-rates in eqn. 1 are eliminated in favor of the extraction ratio and stage number using the counterflow mass ratio $M_{U,N,i}/M_{S,1,i} = \Gamma_i^{N_{SC}+1}$ which is obtained for $N_{SC} = M$ from the recursion relations (see Appendix). At operating conditions which produce the maximum binary separation, the mass ratio of one component equals the reciprocal of the other. For optimal operation we rearrange eqn. 1 to obtain

$$N_{SC} + 1 = \frac{\ln M_{F,h\neq i}/M_{F,i} + \ln P_{U,i}/(1 - P_{U,i})}{\ln \Gamma_i} \quad (3)$$

where $M_{F,i}$ is the mass flow-rate of solute i in the feedstream.

Now we express the extraction ratio in terms of the thermodynamic separation driving force, δ for difficult, optimized separations to obtain the final form of eqn. 3. In a difficult separation, δ is small and either value of the dimensionless migration velocity, u_i, is close to the average of both, $\bar{u} \equiv 1/2(u_1 + u_2)$. Combining the operating condition for an optimal binary separation, $\Gamma_1\Gamma_2 = 1$ (see Appendix), with the definitions for Γ, u_i and δ yields

$$\Gamma_i^2 = 1 + (-1)^{2/i}\left[\delta + \frac{\bar{u}\delta}{1-\bar{u}} + O(\delta^2)\right] \quad (4)$$

Many bioseparations in particular have large solid-phase capacities for which $\bar{u} \ll 1$, so that a good approximation for the extraction ratio when separating closely related solutes is $\Gamma_i^2 \approx 1 + (-1)^{2/i}\delta$. (The error between this approximation and the "real" value of the extraction ratio relative to the average of the two is, neglecting terms second-order or higher in δ

$$\frac{|\Gamma_i^2 - \Gamma_i^{2\,\text{approx}}|}{\frac{1}{2}(\Gamma_i^2 + \Gamma_i^{2\,\text{approx}})} = \frac{\delta\bar{u}}{1 - \bar{u} + (-1)^{2/i}\delta\left[1 - \frac{\bar{u}}{2}\right]} \quad (5)$$

which approaches zero rapidly as δ and $\bar{u}$ become small.)

Finally, for a steady counterflow system operated to give maximum separation of similar solutes, we substitute $\Gamma_i^2 \approx 1 + (-1)^{2/i}\delta$ into eqn. 3 to obtain

$$N_{SC,tot} = 2\left[\frac{2\ln\left[\dfrac{P_{U,i}}{1-P_{U,i}}\right]}{\delta} - 1\right] + 1 \qquad (6)$$

where $N_{SC,tot} \equiv 2N_{SC} + 1$ is the total number of steady counterflow stages in the column. This is the relation we sought.

The equations summarized in Table I relate exit composition, mean residence time and resolution in analogous differential chromatography and steady counterflow systems to column geometry (N and H or N_{SC} and H_{SC}, ϵ_b, ρ_p), equilibrium parameters (α, u) and operating conditions (v or v_{SC}, Γ). For equivalent values of these parameters, separation of two closely related solutes by model chromatographic and counterflow processes can be directly compared.

COMPARING STEADY COUNTERFLOW WITH DIFFERENTIAL CHROMATOGRAPHY

We now examine general expressions to compare optimized counterflow separation of closely related solutes with conventional fixed-bed chromatography. We begin by contrasting the number of stages and processing residence time required by each process to achieve a given resolution. We then estimate the relative volumes of solvent required for two cases: (i) when feedstreams to each system are equally concentrated, and (ii) when mass loading constrains the operation of each system. Finally, we estimate the relative solid-phase requirement in these two cases by comparing columns with identical mass processing rates which produce equally pure products.

Basis of a counterflow advantage

Consider separating two closely related solutes to a predetermined resolution (or fractional purity) by either differential chromatography or steady, solid–liquid counterflow. The equations for resolution in Table I suggest that the number of counterflow stages required to achieve the split increases inversely with the thermodynamic driving force for separation, δ. In contrast, the number of chromatographic plates required increases with the square of the inverse of δ.

Suppose (i) that the same eluent and large-capacity adsorbent are used in both systems so that their equilibrium and transport properties are equal; and (ii) that the systems are operated with equivalent interstitial velocities. Comparing pseudocontinuum formulations of H by Gibbs and Lightfoot [17] and H_{SC} by Ruthven suggests that the height of a counterflow stage is approximately one-half that of a chromatographic plate under these conditions.

In addition to physical requirements, the time necessary to purify solutes by adsorption is a concern. Zhang et al. [34] investigated biological separations and reported that protein degradation by proteolysis, denaturation and other known processes [35,36] increased with processing time. The relations for residence time in Table I suggest a relative ratio for solute processing time, $\bar{t}_F/\bar{t}$, of

$$\frac{\bar{t}_F}{\bar{t}} = \frac{uv}{NH}\frac{(N_{SC,tot}+1)^2 H_{SC}}{8uv_{SC}} \qquad (7)$$

since the bracketed term of $\bar{t}_F$ reduces to $(N_{SC}+1)/2$ for closely related solutes. Assuming that identical resolution is obtained in systems which are operated equivalently gives

$$\frac{\bar{t}_F}{\bar{t}} = \left[\frac{\ln\left(\dfrac{\Phi(2R)}{\Phi(-2R)}\right)}{4R}\right]^2 \qquad (8)$$

This expression suggests that relative solute processing time is approximately equal in differential chromatography and steady counterflow for values of resolution between 0.9 and 1.5.

Three additional observations are in order. First, the number of counterflow stages required in a difficult separation where both solutes tend to partition to the liquid phase ($\bar{u} \sim 1$) increases proportional to $(1 - \bar{u})/\delta$. Thus, the equation for steady counterflow resolution in Table I appears adequately cautious in such a case. Second, eqns. 7 and 8 conservatively estimate the relative solute residence time at *steady state* by using the maximum expected value of $\bar{t}_F$ —the counterflow mean residence time. For values of the extraction ratio much greater or less than unity, the bracketed term in the equation for $\bar{t}_F$ in Table I reduces to unity so that smaller processing times

would be anticipated for counterflow relative to chromatography. Lastly, both Lapidus and Amundson [7] and Ching and Ruthven [37] reported that the time required after start-up to approach steady-state in counterflow was significant and increased with the difficulty of the separation. The transient-response time will influence both physical and temporal requirements of counterflow.

Relative solvent requirement

We estimate relative solvent usage by determining the solvent volume per unit mass required in steady counterflow relative to differential chromatography: $[V_{solv}/m]_{SC}/[V_{solv}/m]_{DC}$. Expressions for comparable systems constrained by feedstream concentration or by load limitation are obtained by calculating respective values of the product-concentration dilution. We conclude by examining viscous effects at high loading.

We evaluate the maximum fluid-phase solute concentration in the first and final plates to estimate chromatographic concentration dilution as $(c_f^{max}|_{N=1})/(c_f^{max}|_{N=N}) = \sqrt{N}$. This form is consistent with work by Snyder [38] which shows that product dilution in isocratic elution increases at the same rate as resolution.

Dilution of stripper-product concentration in steady counterflow is the ratio of feedstream concentration to stripper effluent concentration —$M_{F,i}U/M_{U,N,i}F$ at constant density where M_F is the solute mass flow-rate in the feedstream. Substituting the recursion relation for $y_{N,i}$ and making use of the feedstage accumulation (total solute input to the feedstage divided by solute input by the feedstream) obtained by Klinkenberg [29]

$$\frac{M_{U,e,i} + M_{S,e,i}}{M_{F,i}} = \frac{\Gamma_i + 1}{\Gamma_i^{N_{SC}+1} + 1} \cdot \frac{\Gamma_i^{N_{SC}+1} - 1}{\Gamma_i - 1} \qquad (9)$$

yields for the product dilution

$$\frac{c_F}{c_N} = \frac{1 + \dfrac{1}{\Gamma^{N_{SC}+1}}}{1 + \dfrac{1}{\Gamma}} \frac{U}{F_{U,e}F} \qquad (10)$$

where $F_{U,e}$ is the fraction of i which exits the

feed stage in the fluid phase. Enricher-product dilution is obtained analogously.

Dilution in counterflow is relatively independent of stage number and extraction ratio, varying only in proportion to U/F as is consistent with intuition. At optimized operation, dilution decreases slightly from $2U/F$ for closely related solutes to U/F for considerably easier separations. (Because $\Gamma < 1$ identifies a species whose net flow is toward the enricher exit, it is infinite as $\Gamma \to 0$.) The assumption by Klinkenberg that feed flow-rate is negligible appears to have inconsequential affect on our estimates of dilution.

The volume of solvent required by counterflow to separate closely related solutes relative to chromatography corresponds to the ratio of product concentration dilutions:

$$\frac{\left[\dfrac{V_{solv}}{m}\right]_{SC}}{\left[\dfrac{V_{solv}}{m}\right]_{DC}} = \frac{2U}{F\sqrt{N}} \frac{c_f^{max}|_{N=1}}{c_F} \qquad (11)$$

We have neglected the void volume of solvent in differential chromatography, supposing that periodic injections are made at a frequency high enough to produce non-overlapping, back-to-back pairs of resolved effluent peaks.

For optimized units whose feedstream concentrations are equal, relative solvent requirement varies with U/F and decreases in direct proportion to square root of the number of chromatographic plates necessary to resolve the solutes. Antia and Horváth [39] and Felinger and Guiochon [40] have shown, however, that separation by differential chromatography in systems with non-linear, multicomponent Langmuir isotherms deteriorates at large solute loadings. Ching et al. [41] demonstrated that only diluting a 40:20 (% w/v) monoethanolamine–methanol feedstream could duplicate simulated moving-bed resolution attained at 20:10 (% w/v) due to type-1 non-linearity in the monoethanolamine isotherm.

Suppose that a maximum solute load in chromatography and counterflow is prescribed to avoid degrading the respective separations. Because the largest solute concentration occurs

at the chromatographic inlet and at the counter-flow feedstage in our model systems, we obtain for similar solutes

$$\frac{c_f^{max}\big|_{N=1}}{c_F} = \frac{F}{2U}(N_{SC} + 1) \qquad (12)$$

since the ratio of feedstage to feedstream concentration equals the product of the feedstage accumulation and $(F_{U,e}F)/U$. Hence, where both columns have been constrained comparably due to non-linearities at high loading

$$\frac{\left[\dfrac{V_{solv}}{m}\right]_{SC}}{\left[\dfrac{V_{solv}}{m}\right]_{DC}} = \frac{\ln\left[\dfrac{\Phi(2R)}{\Phi(-2R)}\right]}{2R} \qquad (13)$$

which suggests a relative two-fold increase in counterflow solvent usage for values of resolution between 0.9 and 1.5.

Consider now viscous effects at high sample loading which include viscous fingering observed by Athalye [42] and gross band deformation reported by Yamamoto et al. [43] in differential, size-exclusion chromatography. These occur at local concentration gradients where fast-moving, low-viscosity eluent displaces a viscous solute band. We divide the ratio of the peak fluid-phase solute concentration to its value at n standard deviations from the peak $(z = z_0 + ns)$ by ns to estimate the local chromatographic concentration change as

$$\frac{1}{ns}\frac{c_f^{max}}{c_f\big|_{z=ns}} = \frac{\exp\dfrac{n^2}{2}}{nH\sqrt{N}} \qquad (14)$$

The local counterflow concentration change per stage, estimated in the enricher using the stagewise recursion relation, $y_j/y_e = (\Gamma^j - 1)/(\Gamma^{M+1} - 1)$, is

$$\frac{y_{j+1}}{y_j} = \frac{\Gamma^{j+1} - 1}{\Gamma^j - 1} \qquad (15)$$

Fig. 3 illustrates the magnitude of local dilution in counterflow for two separations with thermo-dynamic driving forces of 0.209 and 0.00209, respectively. Although composition changes (see Fig. 4) are large near column exits and the feed stage, local dilution measured by eqn. 15 is
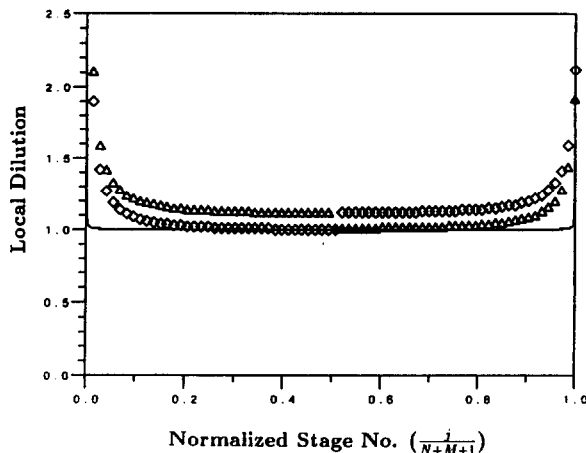

Fig. 3. Local dilution profiles in counterflow for the two separations described in Fig. 4. In the easier separation ($\delta = 0.209$) solute 1 ($\triangle$) partitions preferentially to the upper fluid phase while solute 2 ($\diamondsuit$) tends to the lower solid phase. Similarly, in the more difficult separation ($\delta = 0.00209$) solute 1 is represented by the dashed line and solute 2 by the solid line. In each case, profiles were calculated using stagewise recursion relations for the enricher and stripper with $M = N$ large enough to resolve 1 and 2 to unity ($P_{U,1} = 0.9772$).

Fig. 4. Relative concentration profiles in counterflow for two separations. In the easier separation ($\delta = 0.209$) solute 1 ($\triangle$) partitions preferentially to the upper fluid phase while solute 2 ($\diamondsuit$) tends to the lower solid phase. Similarly, in the more difficult separation ($\delta = 0.00209$) solute 1 is represented by the dashed line and solute 2 by the solid line. In each case, profiles were calculated using stagewise recursion relations for the enricher and stripper with $M = N$ large enough to resolve 1 and 2 to unity ($P_{U,1} = 0.9772$).
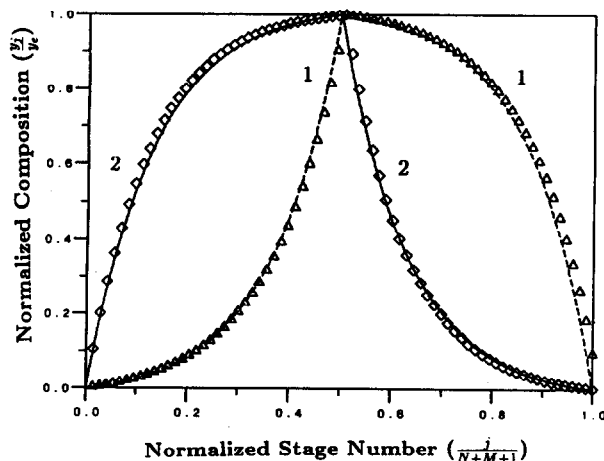
largest in difficult separations for both components near the stripper and enricher exits where relative compositions are relatively small. Dilution values for components 1 and 2 in the larger column are nearly indistinguishable.

Finally, we note that steady counterflow composition profiles (and dilution profiles) plotted for difficult, high-resolution separations using *scaled* variables vary little over two decades of δ, as illustrated in Fig. 4 (and Fig. 3). The appropriate scaling factors $-y_{e,i}$ for stage composition $y_{j,i}$ and $M + 1$ for enricher-stage $j-$ were determined by applying the binomial theorem and counterflow mass ratio to the stagewise recursion relation for solute 1 which partitions preferentially to the liquid to obtain

$$\frac{y_{j,1}}{y_{e,1}} = \frac{2j}{M+1} \cdot \frac{(1 - P_{U,1})^2}{2P_{U,1} - 1} \ln\left[\frac{P_{U,1}}{1 - P_{U,1}}\right]$$
$$\times \left\{ 1 + \frac{(j-1)\delta}{2}\left[1 + \frac{(j-2)\delta}{3}(1 + \cdots) \right] \right\}$$

(16)

Relative solid-phase requirement

We estimate relative solid-phase usage by calculating the ratio of counterflow and chromatography column volumes necessary to produce equally pure products at identical mass processing rates, $M_{U,N,i}/P_{U,i} = m_0/\bar{t}$. For simplicity, the rate at which subsequent injections are made is assumed to be $1/\bar{t}$ and both columns are operated to produce equal interstitial velocities. The column volume ratio is computed for equal feedstream concentrations as well as for comparable load limitations.

In high-resolution separations, average chromatographic effluent concentration is approximately $\bar{c}_f|_{z=L} \approx (m_0 u \sqrt{N})/(A\epsilon_b 6L)$ and counterflow exit concentration is very nearly $c_N \approx y_{N,i}\rho_U$ so that at equal processing rates

$$\frac{c_N}{\bar{c}_f|_{z=L}} = \frac{6}{\sqrt{N}}\frac{Av}{A_{SC}v_{SC}}$$

(17)

We substitute eqn. 11 and multiply the subsequent ratio of cross-sectional areas by a ratio of required lengths. Then N and N_{SC} are eliminated in favor of δ and R to obtain

$$\frac{(2N_{SC} + 1)A_{SC}H_{SC}}{NAH} = \frac{3}{32}\frac{U}{F}\frac{\ln\left[\frac{\Phi(2R)}{\Phi(-2R)}\right]}{R^4}\delta^3$$

(18)

for systems with equal feed concentrations and

$$\frac{(2N_{SC} + 1)A_{SC}H_{SC}}{NAH} = \frac{3}{32}\frac{\ln\left[\frac{\Phi(2R)}{\Phi(-2R)}\right]}{R^4}\delta^2$$ (19)

for systems comparably constrained by load limitations.

Eqns. 18 and 19 suggest that the relative solid-phase requirement is larger for separations involving closely related solutes than for easier, low-δ splits. (The comparative advantage is larger for systems with equal feed concentrations.) The physical basis for the decrease in adsorbent requirement is apparent in a comparison of Figs. 1 and 4 in which binary composition profiles are illustrated for a resolution of unity (a 97.72% mutual separation). Five percent of the fixed bed actively separates 1 from 2 while all of the counterflow column actively resolves the two components.

In Table II the expressions for relative mean residence time and relative solvent and solid-phase requirement for counterflow and chromatographic systems with equal feed concentrations are summarized.

RESULTS AND DISCUSSION

Reported values of dilution, solvent requirement and adsorbent requirement from three simulated moving-bed studies in Table III are compared with corresponding steady counterflow estimates in Table IV. Observed values are well within an order of magnitude of expected results. Approximating fixed-bed dilution by $\sqrt{N}$ yielded values about a factor of six lower than reported dilutions. Consequently, the anticipated relative solvent required to purify racemic 1-phenylethanol was about six times higher than observed. In each case, the estimates of counterflow performance relative to chromatography were conservative.

Note that the sugar-fractionation data repre-

TABLE II

SEPARATION BY STEADY COUNTERFLOW RELATIVE TO DIFFERENTIAL CHROMATOGRAPHY

Relative performance	Expression
Mean residence time	$\dfrac{\bar{t}_F}{\bar{t}} = \left[\dfrac{\ln\left(\dfrac{\Phi(2R)}{\Phi(-2R)}\right)}{4R} \right]^2$
Required solvent volume	$\dfrac{\left[\dfrac{V_{solv}}{m}\right]_{SC}}{\left[\dfrac{V_{solv}}{m}\right]_{DC}} = \dfrac{2U}{F\sqrt{N}}$
Required solid-phase volume	$\dfrac{(2N_{SC}+1)A_{SC}H_{SC}}{NAH} = \dfrac{3}{32}\dfrac{U}{F}\dfrac{\ln\left[\dfrac{\Phi(2R)}{\Phi(-2R)}\right]}{R^4}\delta^3$

sent a linear glucose/Duolite adsorption iso-therm at the concentrations considered (see Ching et al. [28]) while the isotherms of the racemic resolution and lysine recovery were non-linear. The tractable expressions we have derived from counterflow and chromatographic models in which adsorption was presumed linear with a constant equilibrium distribution coefficient approximate the relative performance of both linear and non-linear systems. Previous analyses of non-linear chromatography [15,44] and counterflow [28,41] suggest that more specific comparisons of the relative performance

of non-linear systems (other than specialized Langmuir chromatographic adsorptions for which analytic solutions for concentration profiles have been derived by Thomas [45] and Glueckauf [46]) will likely be limited in scope, and that numerical analysis will probably replace analytic expressions such as ours.

Until more general relations are developed, a detailed analysis of linear systems provides a useful starting point to examine relative performance of counterflow and chromatographic separations. Consider resolution of ovalbumin (OA) and bovine serum albumin (BSA) using

TABLE III

EXPERIMENTAL RESULTS: SIMULATED MOVING-BED (SMB) VS. DIFFERENTIAL CHROMATOGRAPHY (DC)

	Parameters			Reported performance			
	$\dfrac{U}{F}$	H	δ	Dilution		Requirement, SMB/DC	
		(cm)		SMB	DC	Solvent	Adsorbent
Racemic resolution[a]	31	0.015	nr[d]	11.5	290	0.011	0.016
Sugar fractionation[b]	8.5	10	0.27	8.3	22.0	nr	nr
Lysine recovery[c]	1.2	nr	nr	0.79	0.96	0.5	0.1

[a] Ref. 2. Flow-rate and counterflow dilution ratio calculated from values of flow-rate and concentration reported for R-(+)-1-phenylethanol-rich raffinate.
[b] Ref. 52. Flow-rate and counterflow dilution ratio calculated from values of flow-rate and concentration reported for glucose in the post-feed columns of run 4.
[c] Ref. 3. Flow-rate and dilution ratios calculated from arithmatic averages of ranges reported for flow-rates and concentrations.
[d] Not reported.

TABLE IV

CALCULATED RESULTS: STEADY COUNTERFLOW *VS.* DIFFERENTIAL CHROMATOGRAPHY

| | Estimated performance | | | |
| | Dilution | | Requirement, SC/DC | |
	SC^a	DC^b	$Solvent^c$	Adsorbent
Racemic resolution	31	58	0.068	0.017^d
Sugar fractionation	8.5	3.2	13	0.15^e
Lysine recovery	1.2	na^f	na	na

[a] Estimated as U/F since reported concentration profiles suggested $F_{U,e} \sim 1$ in each separation. See *Relative solvent requirement* section.

[b] Estimated as $\sqrt{N}$. See *Relative solvent requirement* section.

[c] Estimated as $U/\sqrt{N}F$. See *Relative solvent requirement* section and footnote a.

[d] Estimated as $(3N_{SC,tot}Uc_f|_{N=1})/(NFc_F)$ with N_{SC} calculated assuming $H \approx 2H_{SC}$ since thermodynamic data for δ were not reported. See *Relative solid-phase requirement* section.

[e] Estimated as $\left(3Uc_f|_{N=1} \ln\left[\dfrac{\Phi(2R)}{\Phi(-2R)}\right]\delta^3\right)/(64Fc_FR^4)$ with $R = 1$. See *Relative solid-phase requirement* section.

[f] Not available, as measured values of H and δ were not reported.

Toyopearl (TSK gel) HW55F ($d_p = 44\ \mu$m). This separation depends on size exclusion, as do fractionation of dextran by Ca^+ resin and "Molex" processes. Parameter values for this case study including those reported by Yamamoto *et al.* [47] and Germershausen *et al.* [48] are summarized in Table V. The relative error of approximating Γ_1 by $1 + \delta$ is 0.076, as determined using eqn. 5. The calculated measures of relative separation performance are listed in Table VI.

Expected solute mean residence times in the two systems are roughly equal. Solvent usage in

counterflow is expected to be less than one quarter of the value required for chromatography, for systems with equal feed concentrations. Due to the low thermodynamic driving force for separation, almost four orders of magnitude less gel filtration resin is required for counterflow relative to fixed-bed separation. In contrast, the anticipated relative solid-phase requirement for less strenuous separations such as fructose/glucose fractionation in Table III is considerably smaller.

Comparing models of counterflow and chromatography suggests that steady counterflow

TABLE V

PARAMETER VALUES FOR SEPARATION OF BOVINE SERUM ALBUMIN (BSA) AND OVALBUMIN (OA) IN TSK HW55F

Parameter	BSA	OA	System
Intraparticle porosity[a], $\epsilon_{p'}$	0.30	0.34	–
Bed void fraction[b], ϵ_b	–	–	0.34
Thermodynamic driving force, δ	–	–	0.048
Required resolution, R	–	–	1.0
Volumetric dilution, U/F	–	–	10

[a] Ref. 47.

[b] Ref. 48.

TABLE VI

SEPARATION OF BOVINE SERUM ALBUMIN AND OVALBUMIN IN TSK HW55F

Steady counterflow *vs.* gel filtration chromatography

Relative performance	Ratio	Value
Required stages	$\dfrac{N_{SC,tot}}{\bar{N}}$	$\dfrac{313}{6975}$
Mean residence time	$\dfrac{\bar{t}_F}{\bar{t}}$	0.883
Required solvent	$\dfrac{[V/m_0]_{SC}}{V/m_0]_{DC}}$	0.239
Required solid-phase	$\dfrac{(2N_{SC}+1)A_{SC}H_{SC}}{NAH}$	0.0004

utilizes stage volumes more efficiently than differential chromatography utilizes plate volumes. For a given resolution, the number of stages required by chromatography to separate close solutes relative to counterflow increases inversely with the thermodynamic driving force for separation. This appears to be the basis for reported order-of-magnitude decreases in adsorbent volume obtained by simulating counterflow in packed beds. Substantial reported reductions in solvent volume may be related to large dilutions observed in chromatography relative to counterflow, whose value is proportional to the square-root of the number of chromatographic stages required to resolve similar products.

Viscous effects such as fingering and gross band deformation are also expected be less problematic in counterflow where local concentration changes are small relative to chromatography. Chromatographic concentration near the inlet changes over an order of magnitude within an axial distance corresponding to one stage, whereas the maximum counterflow change per stage is less than one-fourth that value, as illustrated in Fig. 3. Note that solute composition in counterflow increases in the direction of fluid flow only in the enricher section. So hydrodynamic instabilities reinforced by viscosity differences are not expected to decrease separation efficiency in the stripper.

Simulating counterflow appears particularly advantageous for difficult separations such as resolution of optical isomers or protein variants. In addition to Sorbex-type equipment, the rotating-barrel liquid extractor proposed by Brenner and machines by Ito offer the number of counterflow stages required to separate close solutes. On the other hand, steady operation is limited to binary separations, so equipment must be doubled for ternary systems which are often encountered in present-day chromatography. On balance, progress should be made cautiously, but the potential advantages of counterflow appear attractive enough to deserve a real effort.

SYMBOLS

A	column cross-sectional area (cm^2)
$\bar{c}$	time-averaged fluid-phase solute concentration in chromatography (g/cm^3)
c_f	solute concentration in moving fluid phase in chromatography (g/cm^3)
c_N	solute concentration at the N-stage stripper exit in the upper fluid phase in counterflow (g/cm^3)
$c_{p,i}$	concentration of solute i in phase p in chromatography (g/cm^3)
$D_{p'}$	effective solute diffusivity in pore liquid (cm^2/s)
F	feed mass flow-rate in counterflow (g$_U$/s)
$F_{p,i}$	fractional recovery of species i in phase p
$F_{p,e}$	fraction of a component exiting the feed stage which leaves in phase p
H	height equivalent to a theoretical chromatographic plate (cm)
H_{SC}	height equivalent to one counterflow stage (cm)
k_{ads}	forward rate constant of adsorption (s^{-1})
k_c	concentration-based fluid-phase mass transfer coefficient (cm/s)
k_{des}	rate constant of desorption (s^{-1})
$K_{eq,i}$	ratio of masses of adsorbed and pore-liquid solutes at equilibrium
L	length of chromatographic column ($= HN$) (cm)
m_0	total solute mass which enters chromatography column in a pulse (g)

M	number of stages in the counterflow enricher section
M_F	mass flow-rate of species which enters the counterflow column through the feedstream (g/s)
$M_{p,j}$	mass flow-rate of species leaving stage j in phase p (g/s)
$M_{p,j,i}$	mass flow-rate of species i leaving stage j in phase p (g_i/s)
N	number of stages
$N_{SC,tot}$	total number of stages in a counterflow system
P	purity of species in a chromatographic separation
$P_{p,i}$	fractional purity of species i in phase p
r	fractional relative motion of the lower solid phase
R	chromatographic resolution
R_b	radius of a solid-phase particle (cm)
s^2	variance about the mean (s^2)
s_t	standard deviation normalized by the mean residence time
S	lower solid-phase mass flow-rate (g_S/s)
t	time (s)
$\bar{t}$	mean residence time in chromatography (s)
$\bar{t}_F$	mean residence time in steady counterflow of a component which enters through the feedstream alone
T	transfer rate of one stage volume (s^{-1})
u_i	equilibrium fraction of species i in the fluid phase
U	upper fluid phase mass flow-rate (g_U/s)
v	interstitial velocity in chromatography or equivalent countercurrent interstitial velocity in counterflow (cm/s)
V	volume of solvent
$x_{j,i}$	fraction of the lower solid phase leaving stage j which is species i (g_i/g_S)
$y_{j,i}$	fraction of the upper fluid phase leaving stage j which is species i (g_i/g_U)
z	axial coordinate (cm)
z_0	mean position of a solute peak at a given time, defined as uvt (cm)

Greek letters

α_i	partition coefficient of i between fluid and solid phase
δ	fractional difference in u for two species: thermodynamic driving force for separation
ϵ	convective axial dispersion coefficient (cm^2/s)
ϵ_b	interparticle or column void volume
$\epsilon_{p'}$	intraparticle porosity
Γ_i	extraction ratio of solute i
Λ	selectivity, defined as Γ_1/Γ_2
Φ	cumulative distribution function of the standard normal distribution
ρ_U	density of upper liquid phase (g_U/m^3)
ρ_S	density of lower solid phase (g_S/m^3)
ξ	extent of separation

Subscripts and superscripts

1	enricher exit stage
b	bulk (stationary) phase in chromatography
e	feed stage
f	moving fluid phase in chromatography
F	feedstream
i	species identification subscript
j	stage identification subscript
DC	differential chromatography
N	stripper exit stage
p	phase identification subscript
p'	porous fluid entrained in the bulk phase in chromatography
S	lower solid phase in counterflow
SC	steady counterflow
U	upper liquid phase in counterflow

APPENDIX

Here we provide the derivation of the operating condition for optimum binary counterflow separation utilized in the *Binary counterflow separation* section. We have included this derivation which follows a previous analysis by Rony [49] to elucidate the basis of the relation for binary counterflow separation and to clarify our nomenclature, which differs from his.

Binary counterflow separation produces a difference between fractional recoveries of components 1 and 2 from the fluid stripper effluent and the solid enricher extract. This defines the extent of separation ξ as

D.K. Roper and E.N. Lightfoot / J. Chromatogr. A 654 (1993) 1–16

15

$$\xi \equiv |F_{U,1} - F_{U,2}| = |F_{S,1} - F_{S,2}| \qquad (20)$$

Fractional recovery $F_{p,i}$ of component i from phase p is defined in terms of its flow-rate $M_{p,j,i}$ exiting stage j

$$F_{U,i} \equiv \frac{M_{U,N,i}}{M_{U,N,i} + M_{S,1,i}} \qquad (21)$$

$$F_{S,i} \equiv \frac{M_{S,1,i}}{M_{S,1,i} + M_{U,N,i}} \qquad (22)$$

Species flow-rates are eliminated from eqns. 21 and 22 in favor of N_{SC} and Γ by defining a mass ratio using the recursion relations in Table I

$$\frac{M_{U,N,i}}{M_{S,1,i}} = \frac{y_{N,i} U}{x_{1,i} S} = \frac{\Gamma_i \sum_{j=0}^{M} \Gamma_i^j}{\sum_{k=0}^{N} \Gamma_i^{-k}} \qquad (23)$$

The mass ratio relates exiting compositions without requiring information about the feedstage or feedstream. Using the rule for finite sums of geometric series, $\sum_{j=0}^{n-1} ar^j = [a(1 - r^n)/1 - r]$, the mass ratio for $N = M$ becomes

$$\frac{M_{U,N,i}}{M_{S,1,i}} = \Gamma_i^{N_{SC}+1} \qquad (24)$$

Hence the extraction ratio and the number of counterflow stages completely determine the extent of separation

$$\xi = \left| \frac{1}{1 + \Gamma_1^{-(N_{SC}+1)}} - \frac{1}{1 + \Gamma_2^{-(N_{SC}+1)}} \right| \qquad (25)$$

The value of the extraction ratio which optimizes separation is determined by maximizing ξ in eqn. 25 with respect to Γ_1 after assuming constant selectivity, $\Lambda = \Gamma_1/\Gamma_2$. This results in

$$\Gamma_{i,opt}^{-1} = \Lambda^{\frac{(-1)^i}{2}} \qquad (26)$$

which relates the extraction ratio of component i to a constant ratio of the equilibrium partition coefficients for optimized binary separations. This condition can be used to show that fractional recoveries and fractional purities of solutes in their preferred phase are equal.

The maximum value for the extent of separation is then

$$\xi_{max} = \left| \frac{\Lambda^{(N_{SC}+1)/2} - 1}{\Gamma^{(N_{SC}+1)/2} + 1} \right| \qquad (27)$$

and it is seen that

$$\Gamma_1 \Gamma_2 = 1 \qquad (28)$$

This is the operating condition for optimal separation of a binary mixture. Using the definition of the extraction ratio, a unique, optimum value for the fractional relative solid motion, r, may be determined.

Rony [50] showed that maximum extent of separation in chromatography with optimum distribution ratio was proportional to $\sqrt{N}$. In staged-counterflow with optimum extraction ratio the maximum extent of separation was proportional to N_{SC}. Adjustments to operating conditions and equipment which increase the performance of ideal counterflow separations have been proposed more recently. Liapis and Rippin [5] observed that increasing the column length and number of subdivisions in a simulated moving bed improved the adsorbent utilization. Storti et al. [51] determined countercurrent flow ratios at which solid and desorbent requirement were minimized using characteristic parameters derived from component feed concentrations, then used equilibrium theory to numerically analyze steady, dispersive flow in one- and four-section, non-linear (but constant-selectivity) systems.

ACKNOWLEDGEMENT

REFERENCES

1 D.B. Broughton, R.W. Neuzil, J.M. Pharis and C.S. Brearley, Chem. Eng. Prog., 66 (1970) 70–75.
2 M. Negawa and F. Shoji, J. Chromatogr., 590 (1992) 113–117.
3 G.J. Rossiter and C.A. Tolbert, presented at the AIChE Annual Meeting, Los Angeles, CA, November 17–22, 1991.
4 E.E. Ernst and D.W. McQuigg, presented at the AIChE Annual Meeting, Miami Beach, FL, November 1–6, 1992.

5 A.I. Liapis and D.W.T. Rippin, *AIChE J.*, 25 (1979) 455–460.

6 D.M. Ruthven, *Principles of Adsorption and Adsorption Processes*, Wiley Interscience, New York, 1st ed., 1984.

7 L. Lapidus and N.R. Amundson, *Ind. Eng. Chem.*, 42 (1950) 1071–1078.

8 T. Miyauchi and T. Vermeulen, *Ind. Eng. Chem. Fundam.*, 2 (1963) 113–125.

9 D.M. Ruthven and C.B. Ching, *Chem. Eng. Sci.*, 44 (1989) 1011–1038.

10 U.P. Ernst and J.T. Hsu, presented at the *AIChE Annual Meeting*, Los Angeles, CA, November 17–22, 1991.

11 G. Storti, M. Mazzotti, L.T. Furlan, M. Morbidelli and S. Carra, presented at the *AIChE Annual Meeting*, Miami Beach, FL, November 1–6, 1992.

12 B.B. Fish, R.W. Carr and R. Aris, *AIChE J.*, 35 (1989) 737–745.

13 J.C. Giddings, *Dynamics of Chromatography, Part I, Principles and Theory* (*Chromatographic Science Series*, Vol. 1), Marcel Dekker, New York, 1965.

14 R. Aris and N.R. Amundson, *Mathematical Methods in Chemical Engineering*, Prentice Hall, Englewood Cliffs, NJ, 1973.

15 B. Lin, Z. Ma, S. Golshan-Shirazi and G. Guiochon, *J. Chromatogr.*, 500 (1990) 185–213.

16 J.F.G. Reis, E.N. Lightfoot, P.T. Noble and A.S. Chiang, *Sep. Sci. Technol.*, 14 (1979) 367–394.

17 S.J. Gibbs and E.N. Lightfoot, *Ind. Eng. Chem. Fundam.*, 25 (1986) 490–498.

18 I. Stakgold, *Greens Functions and Boundary Value Problems*, Wiley, New York, 1979.

19 A.M. Athalye, S.J. Gibbs and E.N. Lightfoot, *J. Chromatogr.*, 589 (1992) 71–85.

20 J.J. van Deemter, F.J. Zuiderweg and A. Klinkenberg, *Chem. Eng. Sci.*, 5 (1956) 271–289.

21 P.J. Karol, *Anal. Chem.*, 61 (1989) 1937–1941.

22 J.C. Giddings, *Unified Separation Science*, Wiley, New York, 1991.

23 A. Kremser, *Natl. Pet. News*, 22(21) (1930) 42.

24 M. Souders and G.G. Brown, *Ind. Eng. Chem.*, 24 (1932) 519–522.

25 C.J. King, *Separation Processes*, McGraw-Hill, New York, 2nd ed., 1980.

26 R.E. Treybal, *Mass Transfer Operations*, McGraw-Hill, New York, 3rd ed., 1980.

27 E.J. Henley and J.D. Seader, *Equilibrium-Stage Separation Operations in Chemical Engineering*, Wiley, New York, 1st ed., 1981.

28 C.B. Ching, C. Ho, K. Hidajat and D.M. Ruthven, *Chem. Eng. Sci.*, 42 (1987) 2547–2555.

29 A. Klinkenberg, *Chem. Eng. Sci.*, 1 (1951) 86–92.

30 A. Klinkenberg, H.A. Lauwerier and G.H. Reman, *Chem. Eng. Sci.*, 1 (1951) 93–99.

31 D.K. Roper and E.N. Lightfoot, *Chem. Eng. Sci.*, submitted for publication.

32 B.A. Buffham and H.W. Kropholler, *Chem. Eng. Sci.*, 28 (1973) 1081–1089.

33 R.V. Hogg and J. Ledolter, *Engineering Statistics*, Macmillan, New York, 1st ed., 1987.

34 X. Zhang, R.D. Whitley and N.-H.L. Wang, presented at the *AIChE Annual Meeting*, Los Angeles, CA, November 17–22, 1991.

35 R.K. Scopes, *Protein Purification*, Springer, New York, 1987.

36 W.S. Hancock, S. Wu and J. Frenz, *LC–GC*, 10 (1992) 96–104.

37 C.B. Ching and D.M. Ruthven, *Chem. Eng. Sci.*, 40 (1985) 887–891.

38 L.R. Snyder, in Cs. Horváth (Editor), *High-Performance Liquid Chromatography*, Vol. 1, Academic Press, New York, 1980, pp. 207–316.

39 F.D. Antia and Cs. Horváth, *J. Chromatogr.*, 484 (1989) 1–27.

40 A. Felinger and G. Guiochon, *J. Chromatogr.*, 591 (1992) 31–45.

41 C.B. Ching, C. Ho and D.M. Ruthven, *Chem. Eng. Sci.*, 43 (1988) 703–711.

42 A.M. Athalye, *PhD. Thesis*, University of Wisconsin-Madison, 1993.

43 S. Yamamoto, M. Nomura and Y. Sano, *J. Chem. Eng. Jap.*, 19 (1986) 227–231.

44 T. Gu, G. Tsai and G.T. Tsao, *AIChE J.*, 36 (1990) 784–788.

45 H.C. Thomas, *J. Am. Chem. Soc.*, 66 (1944) 1664.

46 E. Glueckauf, *Proc. R. Soc. London, A*, 186 (1946) 35.

47 S. Yamamoto, M. Nomura and Y. Sano, *J. Chromatogr.*, 394 (1987) 363–387.

48 J. Germershausen, R. Bostedor, R. Liou and J.D. Karkas, *J. Chromatogr.*, 270 (1983) 383–386.

49 P.R. Rony, *Sep. Sci.*, 5 (1970) 1–10.

50 P.R. Rony, *Sep. Sci.*, 5 (1970) 121–135.

51 G. Storti, M. Masi, S. Carra and M. Morbidelli, *Chem. Eng. Sci.*, 44 (1989) 1329–1345.

52 C.B. Ching and D.M. Ruthven, *Chem. Eng. Sci.*, 40 (1985) 877–885.